

## Supplemental Information

### **Supplemental Tables and Figures**

<i>Supplemental Table 1:</i>	Kinetic characterization of wild-type Rv0045c against fluorogenic ester substrates.	S2
<i>Supplemental Table 2:</i>	Biochemical characterization of Rv0045c and Rv0045c loop variants.	S3
<i>Supplemental Table 3:</i>	Substitutions amongst hydrolases similar to Rv0045c.	S4
<i>Supplemental Table 4:</i>	Biochemical characterization of Rv0045c and Rv0045c active site variants.	S5
<i>Supplemental Table 5:</i>	Biochemical characterization of His187 Rv0045c variants against different fluorogenic substrates	S6
<i>Supplemental Table 6:</i>	Biochemical characterization of His187 Rv0045c variants	S7
<i>Supplemental Table 7:</i>	PCR primers used for cloning and site-directed mutagenesis	S8
<i>Supplemental Figure 1:</i>	Protein purification of variants of Rv0045c	S9
<i>Supplemental Figure 2:</i>	Kinetic activity of Rv0045c	S10

Supplemental Table 1: Kinetic characterization of wild-type Rv0045c against fluorogenic ester substrates (Figure 1A, 1B).

Substrate	$k_{\text{cat}}$ ( $10^{-3} \text{ s}^{-1}$ ) <sup>a</sup>	$K_{\text{m}}$ ( $\mu\text{M}$ )	$k_{\text{cat}}/K_{\text{m}}$ ( $\text{M}^{-1} \text{ s}^{-1}$ )
<b>1</b>	0.01 ± 0.001	2.2 ± 0.2	5.0 ± 0.4
<b>2</b>	0.50 ± 0.06	4.0 ± 2.1	120 ± 70
<b>3</b>	0.36 ± 0.02	1.0 ± 0.2	350 ± 90
<b>4</b>	0.10 ± 0.02	2.3 ± 0.1	45 ± 2
<b>5</b>	0.032 ± 0.001	4.4 ± 0.4	7.3 ± 0.7
<b>6</b>	11 ± 1	1.6 ± 0.5	6600 ± 2100
<b>7</b>	1.1 ± 0.1	3.7 ± 1.9	290 ± 150
<b>8</b>	22 ± 1	8.9 ± 1.3	2500 ± 400
<b>9</b>	0.011 ± 0.001	3.3 ± 0.3	3.4 ± 0.3
<b>10</b>	0.006 ± 0.003	0.52 ± 0.08	13 ± 2
<b>11</b>	0.16 ± 0.01	6.8 ± 0.5	24 ± 2
<b>12</b>	0.065 ± 0.003	3.59 ± 0.64	18 ± 3
<b>13</b>	0.40 ± 0.02	8.7 ± 1.1	48 ± 6
<b>14</b>	0.0055 ± 0.0004	1.4 ± 0.3	3.9 ± 1
<b>15</b>	ND <sup>b</sup>	ND	ND
<b>16</b>	0.026 ± 0.002	2.7 ± 0.5	9.8 ± 2.1
<b>17</b>	0.050 ± 0.001	5.6 ± 0.2	8.9 ± 0.3
<b>18</b>	0.011 ± 0.001	4.1 ± 0.2	2.6 ± 0.2
<b>19</b>	0.0020 ± 0.0001	8.5 ± 1.6	270 ± 50
<b>20</b>	ND	ND	ND
<b>21</b>	ND	ND	ND

<sup>a</sup>Kinetic constants for fluorogenic enzyme substrates (Figure 1) were determined by measuring the increase in fluorogenic enzyme substrate fluorescence over time. Data were fitted to a standard Michaelis-Menten equation to determine the values for  $k_{\text{cat}}$ ,  $K_{\text{M}}$ , and  $k_{\text{cat}}/K_{\text{M}}$ . Kinetic measurements for each substrate were repeated three times and the values are given ± SE.

<sup>b</sup>Not determinable. Values were below the detection limit for the assay, determined based on the catalytic activity of S154A Rv0045c.

Supplemental Table 2: Biochemical characterization of Rv0045c and Rv0045c loop variants.

Rv0045c loop variant	$k_{\text{cat}}$ ( $10^{-3} \text{ s}^{-1}$ ) <sup>a</sup>	$K_{\text{m}}$ ( $\mu\text{M}$ )	$k_{\text{cat}}/K_{\text{m}}$ ( $\text{M}^{-1} \text{ s}^{-1}$ )	$T_{\text{m}}$ ( $^{\circ}\text{C}$ ) <sup>b</sup>
WT	$11 \pm 1$	$1.6 \pm 0.5$	$6600 \pm 2100$	$43 \pm 0.5$
Q194A	$0.75 \pm 0.08$	$0.27 \pm 0.16$	$2800 \pm 1700$	$42 \pm 0.5$
R195A	$2.1 \pm 0.1$	$0.34 \pm 0.11$	$6200 \pm 2100$	$42 \pm 0.5$
G196A	$7.2 \pm 0.4$	$0.82 \pm 0.24$	$8700 \pm 2600$	$42 \pm 0.5$
T197A	$3.0 \pm 0.1$	$0.72 \pm 0.13$	$4100 \pm 800$	$43 \pm 0.5$
V198A	$0.45 \pm 0.02$	$0.62 \pm 0.16$	$730 \pm 190$	$43 \pm 0.5$
L200A	$0.29 \pm 0.02$	$0.29 \pm 0.09$	$1000 \pm 300$	$42 \pm 0.5$
M201A	$5.9 \pm 0.5$	$0.87 \pm 0.39$	$6800 \pm 3100$	$42 \pm 0.5$
H202A	$1.1 \pm 0.1$	$0.35 \pm 0.11$	$3200 \pm 1000$	$43 \pm 0.5$
G203A	$0.76 \pm 0.04$	$0.36 \pm 0.10$	$2100 \pm 600$	$43 \pm 0.5$
E204A	$4.2 \pm 0.2$	$0.61 \pm 0.12$	$6900 \pm 1400$	$40 \pm 0.5$

<sup>a</sup>Kinetic constants were determined by measuring the increase in fluorescence over time for Rv0045c or its loop variants against substrate **6** (21). Data were fitted to a standard Michaelis-Menten equation to determine the values for  $k_{\text{cat}}$ ,  $K_{\text{M}}$ , and  $k_{\text{cat}}/K_{\text{M}}$ . Kinetic measurements for each substrate were repeated three times and the values are given  $\pm$  SE.

<sup>b</sup>Values for  $T_{\text{m}}$  were determined by following the change in Sypro Orange fluorescence with increasing temperature. Melting curves were repeated three times for each variant and the  $T_{\text{m}}$  values reported  $\pm$  SE.

Supplemental Table 3: Substitutions among hydrolases similar to Rv0045c.

Part 1: Substitutions in substrate binding and catalytic residues among hydrolases similar to Rv0045c.

Organism	90	92	153	154	155	178	184	187	252	255	282	309	% Identity
<i>M. tuberculosis H37Rv</i>	G	Q	M	S	L	D	L	H	I	F	F	H	-
<i>M. marinum</i>													79
<i>M. ulcerans</i>													78
<i>M. avium</i>													77
<i>M. vanbaalenii</i>							P			G			66
<i>M. rhodesiae</i>							P		F	G			65
<i>M. smegmatis</i>							P		F	G			63
<i>G. polyisoprenivorans</i>							P	A		A			57
<i>R. jostii</i>							H		L	G			52
<i>N. aromatocivorans</i>			A				-	L	D	S	I		25
<i>G. proteobacterium</i>			A		M		-	L	S	S	V		25
<i>A. xylosoxidans</i>	I	G	H		M		-	F	P	A	Y		25
<i>R. slithyformis</i>			A		M		-	A	T	Q	V		24
<i>B. bacteriovorus</i>	L	G	H		M		-	N	V	G	E		22
<i>H. influenzae</i>	L	G	H		M		-	Y	L	L	Y		20
<i>V. cholerae</i>	L	G	H		M		-	Y	V	L	Y		19
<i>E. coli</i>	L	G	H		M		-	Y	V	L	Y		17

Part 2: Substitutions in flexible loop among hydrolases similar to Rv0045c.

Organism	194	195	196	197	198	200	201	202	203	% Identity
<i>M. tuberculosis H37Rv</i>	Q	R	G	T	V	L	M	H	G	-
<i>M. marinum</i>										79
<i>M. ulcerans</i>										78
<i>M. avium</i>		Q								77
<i>M. vanbaalenii</i>		K					V	Q		66
<i>M. rhodesiae</i>		K					V	Q		65
<i>M. smegmatis</i>		M					V	R	E	63
<i>G. polyisoprenivorans</i>	A	R					I	R		57
<i>R. jostii</i>					T		I	N		52
<i>N. aromatocivorans</i>	V	E	R	I		F		T	A	25
<i>G. proteobacterium</i>	V		R	I	I	F		R	R	25
<i>A. xylosoxidans</i>			E	L	R	T	P	A	S	25
<i>R. slithyformis</i>	I	E	R	I	F	F		S	A	24
<i>B. bacteriovorus</i>	E	Y	L	L	N	V	P	S	P	22
<i>H. influenzae</i>	N	G	L	F	A	K	N	A	K	20
<i>V. cholerae</i>	N	G	L	R	A	I	E	E	Q	19
<i>E. coli</i>	A	A	I	N	A	S	E	S	D	17

<sup>a</sup>The amino acid sequence of Rv0045c was aligned using ClustalW <sup>45</sup>. The amino acid numbering corresponds to the amino acid numbering in Rv0045c. The sequences used in the alignment were from *Mycobacterium tuberculosis* H37Rv (NP\_214559.1),



Supplemental Table 4: Biochemical characterization of Rv0045c and Rv0045c active site variants.

Rv0045c active site variant	$k_{\text{cat}}$ ( $10^{-3} \text{ s}^{-1}$ ) <sup>a</sup>	$K_{\text{m}}$ ( $\mu\text{M}$ )	$k_{\text{cat}}/K_{\text{m}}$ ( $\text{M}^{-1}\text{s}^{-1}$ )	$T_{\text{m}}$ ( $^{\circ}\text{C}$ ) <sup>b</sup>
WT	11 ± 1	1.6 ± 0.5	6600 ± 2100	43 ± 0.5
G90A	7.0 ± 0.3	0.95 ± 0.21	7400 ± 1700	46 ± 0.5
Q92A	1.5 ± 0.2	0.64 ± 0.28	2300 ± 1100	38 ± 0.5
M153A	1.7 ± 0.1	0.50 ± 0.15	3500 ± 1100	46 ± 0.5
S154A	0.020 ± 0.001	0.32 ± 0.10	63 ± 19	44 ± 0.5
L155A	1.0 ± 0.5	0.51 ± 0.11	2000 ± 400	37 ± 0.5
D178A	0.20 ± 0.02	0.93 ± 0.43	210 ± 100	36 ± 0.5
L184A	0.64 ± 0.03	0.49 ± 0.08	1300 ± 200	45 ± 0.5
H187A	16 ± 1	1.6 ± 0.3	9900 ± 1900	42 ± 0.5
I252A	4.8 ± 0.3	0.51 ± 0.16	9500 ± 2900	41 ± 0.5
F255A	6.7 ± 0.5	0.14 ± 0.06	4900 ± 2300	41 ± 0.5
F282A	0.19 ± 0.06	0.40 ± 0.06	490 ± 90	40 ± 0.5
H309A	0.062 ± 0.003	0.25 ± 0.11	250 ± 110	38 ± 0.5
G90A H187A	22 ± 2	6.8 ± 1.3	3300 ± 600	45 ± 0.5

<sup>a</sup>Kinetic constants were determined by measuring the increase in fluorescence over time for Rv0045c or its loop variants against substrate **6** (21). Data were fitted to a standard Michaelis-Menten equation to determine the values for  $k_{\text{cat}}$ ,  $K_{\text{M}}$ , and  $k_{\text{cat}}/K_{\text{M}}$ . Kinetic measurements for each substrate were repeated three times and the values are given ± SE.

<sup>b</sup>Values for  $T_{\text{m}}$  were determined by following the change in Sypro Orange fluorescence with increasing temperature. Melting curves were repeated three times for each variant and the  $T_{\text{m}}$  values reported ± SE.

Supplemental Table 5: Biochemical characterization of His187 Rv0045c variants against different fluorogenic substrates.

Rv0045c His187 variant	Fluorogenic Substrate ( $k_{\text{cat}}/K_{\text{m}}$ ( $\text{M}^{-1}\text{s}^{-1}$ ))				
	<b>3</b>	<b>6</b>	<b>13</b>	<b>14</b>	<b>18</b>
WT	100 ± 40	6600 ± 2100	4.9 ± 2.0	12 ± 1	6.7 ± 0.8
G90A	250 ± 100	7400 ± 1700	27 ± 6.6	17 ± 2	25 ± 5
H187A	650 ± 80	9900 ± 1900	39 ± 8	17 ± 4	9.0 ± 0.5
H187Y	2100 ± 800	53000 ± 6000	110 ± 10	22 ± 4	22 ± 4
G90A/H187A	20 ± 2	3300 ± 600	3.6 ± 0.4	2.6 ± 0.1	4.6 ± 0.8

<sup>a</sup>Kinetic constants were determined by measuring the increase in fluorescence over time for Rv0045c or its catalytic variants against various substrates (Figure 1) (21). Data were fitted to a standard Michaelis-Menten equation to determine the values for  $k_{\text{cat}}$ ,  $K_{\text{M}}$ , and  $k_{\text{cat}}/K_{\text{M}}$ . Kinetic measurements for each substrate were repeated three times and the values are given ± SE.

Supplemental Table 6: Biochemical characterization of His187 Rv0045c variants.

Rv0045c His187 variant	$k_{\text{cat}}$ ( $10^{-3} \text{ s}^{-1}$ ) <sup>a</sup>	$K_{\text{m}}$ ( $\mu\text{M}$ )	$k_{\text{cat}}/K_{\text{m}}$ ( $\text{M}^{-1}\text{s}^{-1}$ )	$T_{\text{m}}$ ( $^{\circ}\text{C}$ ) <sup>b</sup>
WT	11 ± 1	1.6 ± 0.5	6600 ± 2100	43 ± 0.5
H187D	3.9 ± 0.2	1.4 ± 0.3	2900 ± 600	39 ± 0.5
H187F	6.8 ± 0.2	3.2 ± 0.3	2200 ± 200	41 ± 0.5
H187G	13 ± 1	1.4 ± 0.2	8200 ± 2200	39 ± 0.5
H187K	6.9 ± 0.3	2.2 ± 0.5	3200 ± 700	39 ± 0.5
H187N	2.0 ± 0.1	1.0 ± 0.1	1900 ± 300	40.5 ± 0.8
H187P	0.90 ± 0.01	0.60 ± 0.43	1400 ± 1000	41 ± 0.5
H187S	5.4 ± 0.2	0.60 ± 0.10	9100 ± 1500	39 ± 0.5
H187V	10 ± 1	1.6 ± 0.8	6200 ± 2900	40 ± 0.5
H187W	14 ± 1	6.0 ± 1.7	2400 ± 700	43 ± 0.5
H187Y	11 ± 1	0.21 ± 0.03	53000 ± 6000	41.5 ± 0.8

<sup>a</sup>Kinetic constants were determined by measuring the increase in fluorescence over time for Rv0045c or its loop variants against substrate **6** (21). Data were fitted to a standard Michaelis-Menten equation to determine the values for  $k_{\text{cat}}$ ,  $K_{\text{M}}$ , and  $k_{\text{cat}}/K_{\text{M}}$ . Kinetic measurements for each substrate were repeated three times and the values are given ± SE.

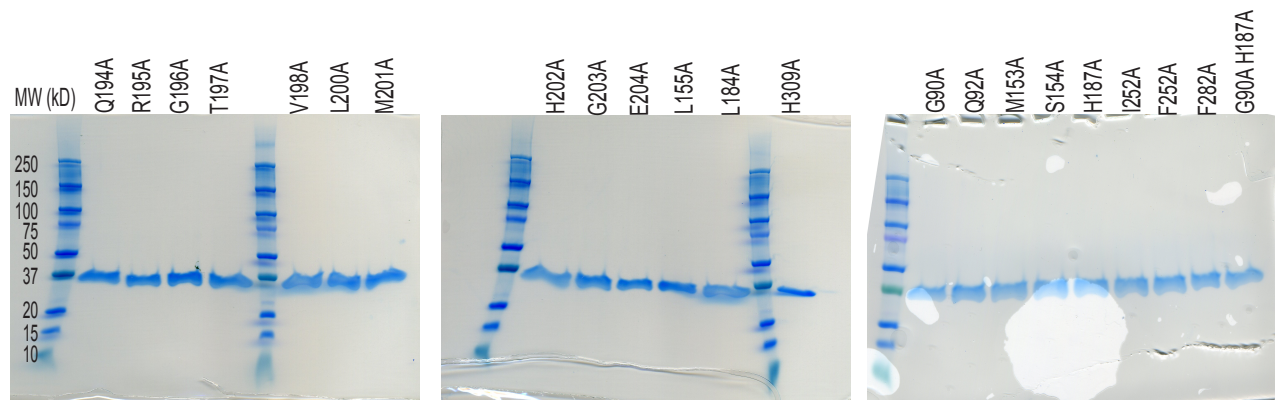
<sup>b</sup>Values for  $T_{\text{m}}$  were determined by following the change in Sypro Orange fluorescence with increasing temperature. Melting curves were repeated three times for each variant and the  $T_{\text{m}}$  values reported ± SE.

Supplemental Table 7: PCR primers used for cloning and site-directed mutagenesis.<sup>a</sup>

Rv0045c Variant	Primer nucleotide sequence
G90A	5'-GGT GAT CTT TCT GCA CGG CGC CGG ACA GAA CGC CCA TAC C-3'
Q92A	5'-CTG CAC GGC GGC GGA GCG AAC GCC CAT ACC TGG G-3'
M153A	5'-GCC GAA TTC GTG GTC GGC GCG TCG CTG GGC GGG TTG-3'
S154A	5'-GCC GAA TTC GTG GTC GGC ATG GCG CTG GGC GGG TTG ACT GCG-3'
L155A	5'-CGT GGT CGG CAT GTC GGC GGC GGG CGG GTT GAC TGC G-3'
D178A	5'- CGG CGA ACT CGT TCT CGT CGC CGT CAC CCC GTC GGC ATT GC-3'
L184A	5'- CGT CAC CCC GTC GGC AGC GCA ACG GCA CGC CGA GC-3'
H187A	5'- CCG TCG GCA TTG CAA CGG GCC GCC GAG CTG ACC GCC G-3'
H187D	5'-CCG TCG GCA TTG CAA CGG GAC GCC GAG CTG ACC GCC G-3'
H187F	5'-CCG TCG GCA TTG CAA CGG TTC GCC GAG CTG ACC GCC G-3'
H187G	5'-CCG TCG GCA TTG CAA CGG GGC GCC GAG CTG ACC GCC G-3'
H187K	5'-CCG TCG GCA TTG CAA CGG AAG GCC GAG CTG ACC GCC G-3'
H187N	5'- CCG TCG GCA TTG CAA CGG AAC GCC GAG CTG ACC GCC G-3'
H187P	5'-CCG TCG GCA TTG CAA CGG CCC GCC GAG CTG ACC GCC G-3'
H187S	5'-CCG TCG GCA TTG CAA CGG AGC GCC GAG CTG ACC GCC G-3'
H187V	5'-CCG TCG GCA TTG CAA CGG GTC GCC GAG CTG ACC GCC G-3'
H187W	5'- CCG TCG GCA TTG CAA CGG TGG GCC GAG CTG ACC GCC G-3'
H187Y	5'-CCG TCG GCA TTG CAA CGG TAT GCC GAG CTG ACC GCC G-3'
Q194A	5'-CCG AGC TGA CCG AGG CGC GCG GCA CGG TGG CG-3'
R195A	5'-GAG CTG ACC GCC GAG CAG GCC GGC ACG GTG GCG C-3'
G196A	5'-ACC GCC GAG CAG CGC GCC ACG GTG GC-3'
T197A	5'-GCC GAG CAG CGA GGT GCA GTG GCG CTG ATG CAC GG-3'
V198A	5'-CGC GGC ACG GCT GCG CTG ATG CAC GGC G-3'
L200A	5'-GGC ACG GTG GCG GCA ATG CAC GGC GAG CGG-3'
M201A	5'-GCG GCA CGG TGG CGC TGG CAC ACG GC-3'
H202A	5'-GCA CGG TGG CGC TGA TGG CGG GCG AGC GGG AAT TCC-3'
G203A	5'-GGT GGC GCT GAT GCA CGC CGA GCG GGA ATT CCC C-3'
E204A	5'-GCG CTG ATG CAC GGC GCG CGG GAA TTC CCC-3'
I252A	5'- GGG TGT GGC GCT ATG ACG CGG CCC GCA CGT TCG GAG ATT TCG C-3'
F255A	5'- GAC GCG ATC CGC ACG GCC GGA GAT TTC GC-3'
F282A	5'- GCG CGG CGG CTC GTC GGG CGC AGT CAC CGA CCA GGA CAC CGC-3'
H309A	5'- CGT CGA GAA GTC AGG CGC CTC GGT GCA AAG TGA CC-3'

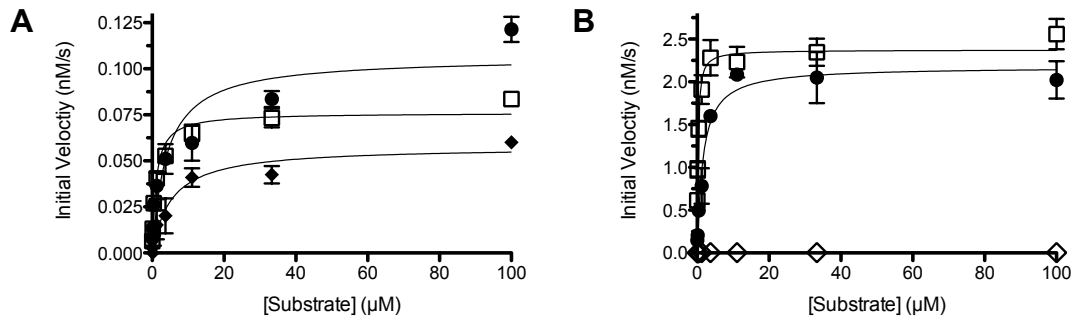
<sup>a</sup>Primers for mutagenesis are one of the two complementary primers used in the mutagenesis reaction. Mutagenic PCR reactions were subjected to the following thermal cycle using a BIO-RAD MyCycler™: 1) initial denaturation at 95°C for 30 s, 2) denaturation at 95°C for 30 s, 3) annealing at temperatures between 52 – 60°C for 60 s, 4) extension at 68°C for 14 min. Steps 2-4 were repeated 16 times.

## Supplemental Figure 1



**Supplemental Figure 1: Protein purification of variants of Rv0045c.** Each Rv0045c variant was constructed and purified as described in the Experimental Section. The expected molecular weight of Rv0045c is 35.5 kDa. Each variant (2  $\mu$ g) was loaded onto the 4-20% Tris-glycine gel and run at 150 V for 45 minutes. The molecular weight was confirmed by comparison to the Kaleidoscope prestained protein standard (Bio-rad laboratories).

## Supplemental Figure 2



**Supplemental Figure 2: Kinetic activity of Rv0045c. A)** Kinetic activity of wild-type Rv0045c against substrates 2 (closed circles), 3 (open squares), and 4 (closed diamonds). All measurements were completed in triplicate and shown  $\pm$  SE. Data were fitted to the Michaelis-Menten equation using Graphpad Prism 5.0. **B)** Kinetic activity of Rv0045c variants. The kinetic activity of S154A (open diamonds), H187A (closed circles), and H187Y (open squares) were determined and plotted the same as part A.